Rock Mech Rock Eng (2017) 50:1055–1061
DOI 10.1007/s00603-016-1139-1

TECHNICAL NOTE

Proposing Triangulation-Based Measures for Rock Fracture Roughness

Nima Babanouri[1] · **Saeed Karimi Nasab**[2]

Received: 27 February 2016 / Accepted: 18 November 2016 / Published online: 25 November 2016

Keywords Surface triangulation · Rock fractures · Roughness scale · Anisotropy

List of symbols

$\boldsymbol{t}$	Shear direction vector
θ	Triangle dip
α	Triangle azimuth
$\boldsymbol{d}$	True dip vector of triangle
$\boldsymbol{w}$	Projection of triangle true dip vector on shear plane
θ^*	Triangle apparent dip in shear direction
A_0	Maximum possible contact area in shear direction
A_{θ^*}	Area of triangles with apparent dip greater than a given value of θ^*
$\theta^*_{\max}$	Maximum apparent dip in shear direction
C	Fitting parameter in Grasselli's model
Δ	Area-weighted mean of apparent dip
$\boldsymbol{a}$	Area vector of triangle
a	True area of triangle
n	Total number of triangles
m	Number of triangles dipping against shear direction
Δ_T	True-area-weighted mean of apparent dip
a_i^*	Apparent area of triangle
Δ_A	Apparent-area-weighted mean of apparent dip
a_i^N	Normal area of triangle
Δ_N	Normal-area-weighted mean of apparent dip
Δ^*	Root area-weighted mean square of apparent dip
Δ_T^*	Root true-area-weighted mean square of apparent dip
Δ_A^*	Root apparent-area-weighted mean square of apparent dip
Δ_N^*	Root normal-area-weighted mean square of apparent dip
Δ^S	Root-mean-squared elevation of involved triangles with respect to best-fit plane
z^C	Elevation of triangle center
$\bar{z}$	Elevation of best-fit plane

1 Introduction

Small changes in rock fracture characteristics may lead to significant changes in the calculated safety factor of rock structures, including different types of surface and underground excavations (Babanouri et al. 2011). Among the influencing parameters, the morphology of rock fracture surfaces is of particular importance in the mechanical and hydraulic behavior of rock masses. Therefore, many methods have been proposed to quantify the roughness of rock discontinuities. Most of the available methods summarize the surface roughness in terms of empirical parameters (Barton and Choubey 1977; Beer et al. 2002), statistical parameters (Tse and Cruden 1979; Yang et al. 2001; Babanouri et al. 2013), or fractal parameters (Odling 1994; Kulatilake et al. 1997; Babanouri et al. 2013), which are usually calculated for two-dimensional profiles of the fracture surface. However, the study of rock fracture roughness can be conducted through a comprehensive three-dimensional (3D) modeling of the surface geometry (Marache et al. 2002; Grasselli et al. 2002; Grasselli 2006; Saito and Grasselli 2010). For this purpose, some attempts

✉ Nima Babanouri
babanouri@hut.ac.ir

[1] Department of Mining Engineering, Hamedan University of Technology, 65155-579 Hamedan, Iran

[2] Department of Mining Engineering, Shahid Bahonar University of Kerman, Kerman, Iran

have been made to describe and reconstruct the morphology of rock discontinuities using geostatistical tools (Marache et al. 2002; Saito and Grasselli 2010; Babanouri and Karimi Nasab 2015). Grasselli introduced a three-dimensional measure of roughness based on analyzing the triangular irregular network (TIN) of the fracture surface which realistically reflects the roughness features (Grasselli et al. 2002; Grasselli 2006).

However, the Grasselli's roughness parameter is quite difficult to calculate, and its physical meaning is unclear. In addition, this measure of roughness is incapable of capturing the scale of roughness. In this study, a series of new TIN-based measures of roughness have been proposed which are easily calculated and carry explicit physical meanings. The suggested measures were then calculated for three natural rock fractures and were compared with the values obtained from the Grasselli's metric.

2 Morphological Data

We measured the surface topography of three natural fractures collected during the work of Amiri Hossaini et al. (2014). The fractures were taken from the Gol-e-Gohar iron ore mine (Iran) with surfaces of high, medium and low roughness, which are, respectively, referred to as S1, S2 and S3 hereafter.

The morphology of the surfaces was scanned using an advanced topometric sensor (ATS) system. The ATS systems provide an optical method based on a combination of white light fringe projection, triangulation and phase shifting for fast and accurate calculation of high-dense 3D point clouds (Bergmann et al. 1997; Grasselli 2001, 2006; Grasselli et al. 2002). The resolution of the collected topography data was 0.05 mm in the x- and y-directions, with an accuracy of up to 2 μm for the elevation (z) measurements.

3 Surface Triangulation

A cloud of points obtained by measurement is not suitable for analyzing the surface roughness and needs to be meshed into a TIN. Various algorithms have been presented for surface triangulation among which the Delaunay method is widely accepted for reconstruction of a surface from a point could. Hence, this method has been used in this study. The Delaunay algorithm connects every point in the point cloud to its natural neighbors and forms a continuous surface of triangles. In other words, circumcircle of a triangle must not surround any other point in the Delaunay triangulation. The Delaunay triangulation maximizes the minimum value of all the angles of the triangles; hence, slender triangles are avoided. A surface triangulation using the Delaunay method

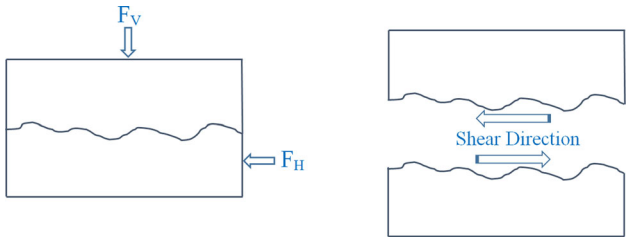

Fig. 1 Convention used for the shear direction on a fracture surface

is unique and independent of choosing the starting point (De Berg et al. 2000).

In this paper, the direction of shearing on a fracture surface is considered as the direction toward which the asperities experience shear force (Fig. 1). In contrast, some references have considered the shear direction on a fracture surface as the direction of its shear displacement relative to the mated surface. Since the shearing direction, in terms of being forward or reverse, would be important in the following TIN-based description of roughness, it was necessary to specify the convention used for the shearing direction on a fracture surface.

4 Grasselli's Roughness Measure

To analyze a triangulated fracture surface, a shear direction ($\boldsymbol{t}$) needs to be considered at first. Each triangle is identified by its dip (θ) and azimuth (α). The dip is the maximum angle between the best-fit plane and the triangle, and the azimuth is considered as the angle between the shear direction and the projection of the true dip vector ($\boldsymbol{d}$) on the shear plane ($\boldsymbol{w}$), measured clockwise from $\boldsymbol{t}$ as illustrated in Fig. 2. The apparent dip (θ^*) is determined by projecting the true dip vector onto the vertical plane passing the shear direction (Fig. 2). The relationship between the apparent dip and true dip is as follows:

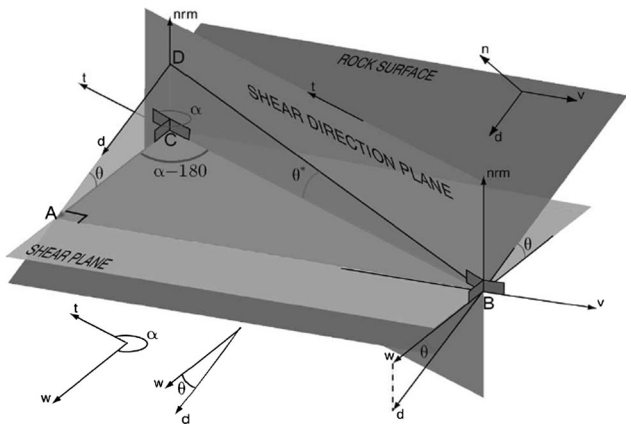

Fig. 2 Geometrical definition of azimuth, dip and apparent dip in the analysis direction (Grasselli et al. 2002)

$$\tan\theta^* = -\tan\theta \times \cos\alpha \quad (1)$$

Grasselli stated that only the triangles dipping against the shear direction (according to Fig. 4) are involved in shear strength mobilization. The maximum possible contact area in the shear direction (A_0) is then calculated as the summation of the areas of the involved triangles. Considering the sum of the area of the involved triangles whose apparent dip in the shear direction is greater than a given value of θ^*, the parameter of A_{θ^*} will be calculated.

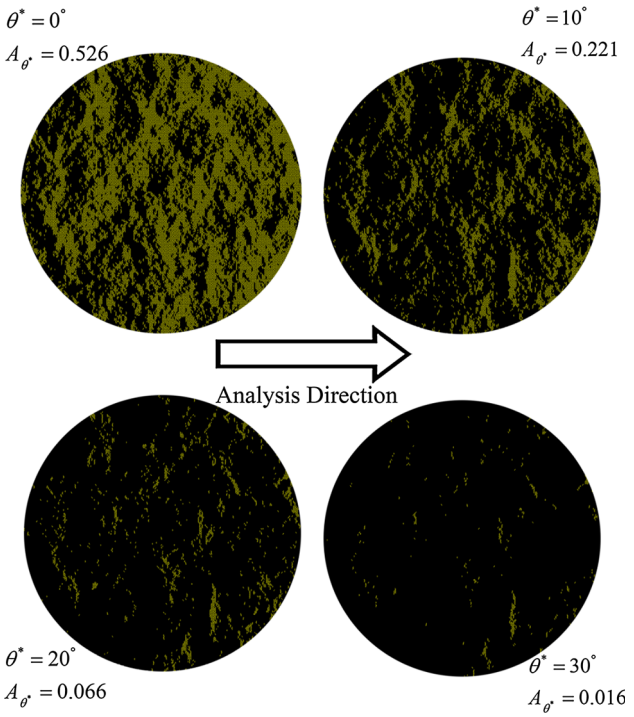

Fig. 3 Contact areas of surface S2 specified in light color for different values of θ^*

In Fig. 3, the areas of the surface S2 in which the apparent dip of the involved asperities in shear direction is greater than $\theta^* = 0°$, 10°, 20° and 30° are specified in light color. If the values of A_{θ^*} are calculated for several values of θ^*, a plot of $A_{\theta^*} - \theta^*$ is achieved (Fig. 4). Grasselli described the relationship between θ^* and A_{θ^*} as follows:

$$A_{\theta^*} = A_0\left(\frac{\theta^*_{\max} - \theta^*}{\theta^*_{\max}}\right)^C, \quad (2)$$

where $\theta^*_{\max}$ is the maximum apparent dip in the analysis direction, and C is a dimensionless coefficient obtained by a nonlinear least-squares regression which characterizes the distribution of the apparent dip angles over the surface. Based on a strong correlation observed between the ratio of $\theta^*_{\max}/C$ and shear strength of rock fractures, $\theta^*_{\max}/C$ was introduced as a measure of surface roughness (Grasselli et al. 2002).

As can be seen in Fig. 4, the TIN-based approach is able to distinguish between the roughness in forward and reverse directions. This advantage, which is referred to as the "one-way roughness description" in here, is barely found in classic methods of roughness description.

Nevertheless, experimental observations were the only basis of accepting the roughness parameter of $\theta^*_{\max}/C$. The justification of why this parameter is correlated with the shear strength was unclear. Recently, the parameter of $\theta^*_{\max}/(C+1)$ was suggested instead of $\theta^*_{\max}/C$ (Tatone and Grasselli 2009). Given the variation range of $[0,\infty]$ for C, the value of $\theta^*_{\max}/(C+1)$ varies from 0 for a completely smooth surface to $\theta^*_{\max}$, for a saw-tooth surface with a consistent inclination anywhere between 0° and 90°. When the values of A_0 differ significantly in forward and reverse directions, the value of A_0 may need to accompany $\theta^*_{\max}/(C+1)$ to completely characterize the roughness anisotropy (Tatone and Grasselli 2009).

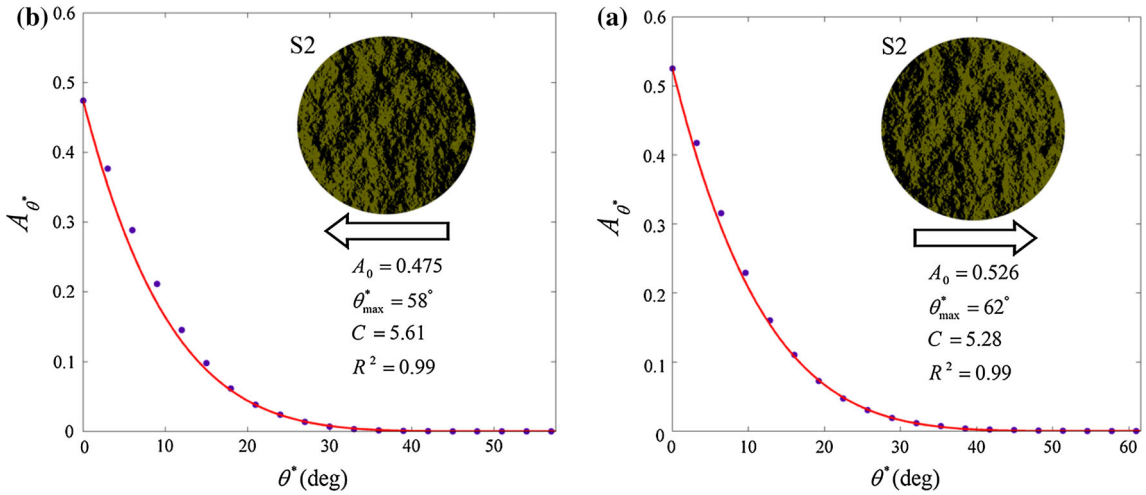

Fig. 4 Plot of A_{θ^*} versus θ^* for surface S2 in forward direction (**a**) and reverse direction (**b**)

5 Proposed TIN-Based Measures of Roughness

The Grasselli's roughness parameter is a 3D measure of rock fracture roughness capable of accurate characterization of anisotropy. However, the calculation of this parameter is associated with difficulties which mainly limit its application to research purposes. To obtain the parameter of C, it is first required to consider multiple values of apparent dip (θ^*) in the shear direction, and calculate their corresponding contact areas (A_{θ^*}). Then, a nonlinear regression, which is associated with uncertainties especially in relation to choosing the initial value, needs to be used for estimating C according to Eq. (2). Therefore, the code required to calculate the Grasselli's roughness parameter is relatively complex, time-consuming, having several loops and iterative computations. In addition, the measure of C is basically empirical, and its physical concept is quite intangible to imagine.

In this study, a number of TIN-based measures of roughness are suggested which are far easier to calculate and have explicit physical meaning. The developed parameters are based on the assumption that the share of triangles in strength mobilization is proportional to their apparent dip as well as their area. In a triangulated surface, only the triangles are considered to be involved shearing which dip against the shear direction. Accordingly, a new parameter of "area-weighted mean of apparent dip" (Δ) is defined. Depending on which component of the triangle area is considered to weight the apparent dip, different versions of Δ can be defined. The area vector ($\boldsymbol{a}_i$) of each triangle is considered to be a vector normal to the triangle with the magnitude of its true area (a_i), as illustrated in Fig. 5. Let n be the total number of triangles of a digitized fracture surface, m be the number of triangles dipping against the shear direction, and θ_i^* be the apparent dip of the involved triangles in the shear direction with respect to the best-fit plane, then:

$$\Delta_T = \frac{\sum_{i=1}^{m} a_i \theta_i^*}{\sum_{i=1}^{m} a_i}, \tag{3}$$

where the index of "T" stands for being weighted by the true area. The parameter of Δ_T incorporates the azimuth of each triangle relative to the shear direction only into the dip value not into the weights (i.e., the area values). If the apparent dip is weighted by the apparent area (i.e., a_i^* in Fig. 5), which is considered as the projection of the area vector onto the vertical plane passing through the shear direction, the measure of Δ_A will be obtained:

$$\Delta_A = \frac{\sum_{i=1}^{m} a_i^* \theta_i^*}{\sum_{i=1}^{m} a_i^*}. \tag{4}$$

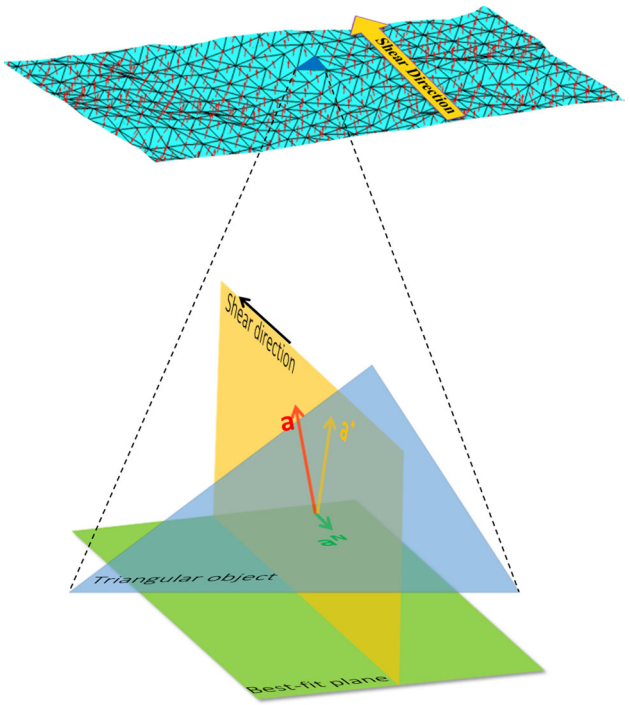

Fig. 5 Geometrical definition of apparent and normal area vectors respect to the shear direction

The measure of Δ_A incorporates the azimuth of triangles not only into the dip value but also into the weight value. If the normal area (i.e., a_i^N in Fig. 5), which is the projection of the area vector in the shear direction, is considered as the weight, the measure of Δ_N is calculated:

$$\Delta_N = \frac{\sum_{i=1}^{m} a_i^N \theta_i^*}{\sum_{i=1}^{m} a_i^N}. \tag{5}$$

The parameter of Δ_N incorporates both the apparent dip of the triangle and its relative azimuth into the weight.

On the other hand, Yang and Chiang (2000) demonstrated that the behavior of a fracture surface composed of asperities of different dips is mainly controlled by the steepest ones (Yang and Chiang 2000). Therefore, it is a reasonable idea to assign greater weights to the steeper asperities of the surface in roughness description. Hence, the operator of root-mean-square (RMS) was used instead of arithmetic average in the followings. Each sample is weighted by its value in the RMS calculation. Therefore, the triangles of higher apparent dip take greater weights in the obtained mean value. Accordingly, the measure of "root area-weighted mean square of apparent dip" (Δ^*) is introduced. Similar to Δ, different versions of Δ^* can be defined depending on considering the true area, apparent area, or normal area of triangles, which are, respectively, shown by Δ_T^*, Δ_A^* and Δ_N^*:

$$\Delta_T^* = \sqrt{\frac{\sum_{i=1}^{m} a_i (\theta_i^*)^2}{\sum_{i=1}^{m} a_i}}, \quad (6)$$

$$\Delta_A^* = \sqrt{\frac{\sum_{i=1}^{m} a_i^* (\theta_i^*)^2}{\sum_{i=1}^{m} a_i^*}}, \quad (7)$$

$$\Delta_N^* = \sqrt{\frac{\sum_{i=1}^{m} a_i^N (\theta_i^*)^2}{\sum_{i=1}^{m} a_i^N}}. \quad (8)$$

The calculation of the parameters of Δ and Δ^* is explicit, fast, and without iterative computations or curve fitting. The impact of shear direction, dip of asperities, as well as their area is taken into account in the roughness

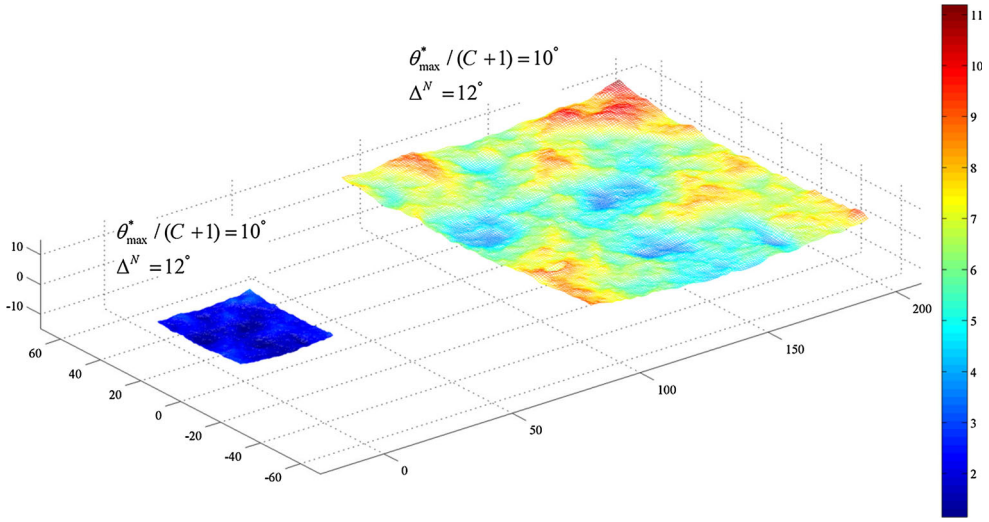

Fig. 6 Ignorance of the roughness scale by texture parameters

Table 1 Values of the TIN-based measures obtained for surfaces of S1, S2 and S3 in different directions

Surface	Direction	A_0 [–]	$\theta^*_{max}/(C+1)$ [°]	Δ_T [°]	Δ_A [°]	Δ_N [°]	Δ_T^* [°]	Δ_A^* [°]	Δ_N^* [°]	Δ^S [mm]
S1	0	0.54	12.02	12.15	15.15	14.63	17.18	19.96	22.08	0.98
	45	0.52	10.21	10.83	13.86	13.52	16.13	19.01	21.37	0.96
	90	0.48	10.33	11.04	14.14	13.65	16.34	19.28	21.90	0.94
	135	0.48	11.67	11.79	15.02	14.08	16.85	19.85	22.52	0.91
	180	0.46	11.68	11.93	15.80	14.82	18.33	22.14	25.74	0.91
	225	0.48	10.65	11.00	14.58	13.83	17.02	20.51	23.80	0.93
	270	0.52	10.03	11.13	14.08	13.68	16.21	18.98	21.31	0.95
	315	0.52	12.96	12.83	15.92	15.34	17.91	20.70	22.78	0.98
S2	0	0.53	9.74	10.08	13.06	12.48	15.13	18.11	20.60	0.46
	45	0.50	9.84	10.17	13.07	12.50	15.00	17.82	20.02	0.45
	90	0.50	9.58	9.91	12.67	12.18	14.58	17.29	19.38	0.45
	135	0.50	8.85	9.69	12.32	11.90	14.18	16.75	18.76	0.43
	180	0.47	8.87	9.69	12.20	11.82	13.98	16.39	18.27	0.43
	225	0.50	8.83	9.47	11.92	11.57	13.66	16.00	17.82	0.43
	270	0.50	8.99	9.52	12.13	11.74	14.02	16.58	18.68	0.44
	315	0.50	9.60	10.02	12.86	12.26	14.72	17.49	19.75	0.45
S3	0	0.52	5.41	5.50	7.21	6.91	8.45	10.29	11.82	0.26
	45	0.59	5.22	5.80	7.39	7.06	8.46	10.11	11.52	0.26
	90	0.59	6.14	6.86	8.54	7.99	9.46	11.15	12.55	0.26
	135	0.56	6.16	6.56	8.26	7.78	9.26	10.97	12.38	0.25
	180	0.48	5.52	5.65	7.66	7.29	9.17	11.46	13.51	0.25
	225	0.41	6.35	6.56	9.13	8.42	10.85	13.83	16.25	0.25
	270	0.41	7.57	7.69	10.39	9.46	11.92	14.87	17.12	0.25
	315	0.44	6.93	7.00	9.32	8.58	10.64	13.12	15.01	0.25

quantification. In addition, the physical concept of the suggested measures is clearly understandable.

The scale of roughness is an important feature of the fracture surface which is reflected neither in the Grasselli's measure nor in the Δ and Δ^* parameters. For instance, Fig. 6 shows two fracture surfaces, one of which is the product of enlarging the other one. None of the introduced TIN-based measures is capable of distinguishing between these two surfaces. The Grasselli's measure and the measures of Δ and Δ^* assess the both surfaces as the same, because they describe the dip of asperities (not their scale) and are in units of angle. At least a pair of parameters, comprising a parameter having units of length to capture the scale and a parameter to describe the roughness texture, is required to sufficiently characterize a rock fracture surface (Babanouri et al. 2013). Thus, a TIN-based parameter reflecting the roughness scale is proposed in this study. The parameter of Δ^S is defined as the RMS of height of the center of the involved triangles with respect to the best-fit plane:

$$\Delta^S = \sqrt{\sum_{i=1}^{m} (z_i^C - \bar{z}_i)^2}, \tag{9}$$

where z_i^C $(i = 1 - m)$ is the elevation of the triangle center, and $\bar{z}_i$ is the elevation of the best-fit plane. The values of the TIN-based measures calculated for the natural rock fracture surfaces of S1, S2 and S3 in different directions are given in Table 1 and illustrated in Fig. 7 as polar plots.

As can be seen from Table 1, and already stated by Grasselli (Grasselli et al. 2002), the value of A_0 for the forward and reverse directions are calculated nearly the same and around 0.5. It is important to note that the value of the Grasselli's measure is found to be nearly equal to the Δ_T value.

6 Conclusions

In this study, a series of TIN-based measures of roughness were introduced which reflect different aspects of rock fracture morphology such as scale, texture and anisotropy. The proposed roughness measures are far easier to calculate and simpler to understand, compared to the available triangulation-based parameters.

A new roughness parameter was developed as the "area-weighted mean of apparent dip" (Δ). Depending on which component of the triangle area is considered to weight the apparent dip, different versions of Δ can be defined.

On the other hand, the parameter of "root area-weighted mean squares of apparent dip" (Δ*) was introduced to dedicate greater weights to the steeper asperities of the surface. The scale of roughness is an important feature of the fracture surface which has been neglected in the TIN-based roughness parameters. Thus, a TIN-based parameter reflecting the roughness scale has been proposed in this study. The parameter of Δ^S is defined as the RMS of height of the center of the involved triangles with respect to the best-fit plane. Finally, the values of the TIN-based

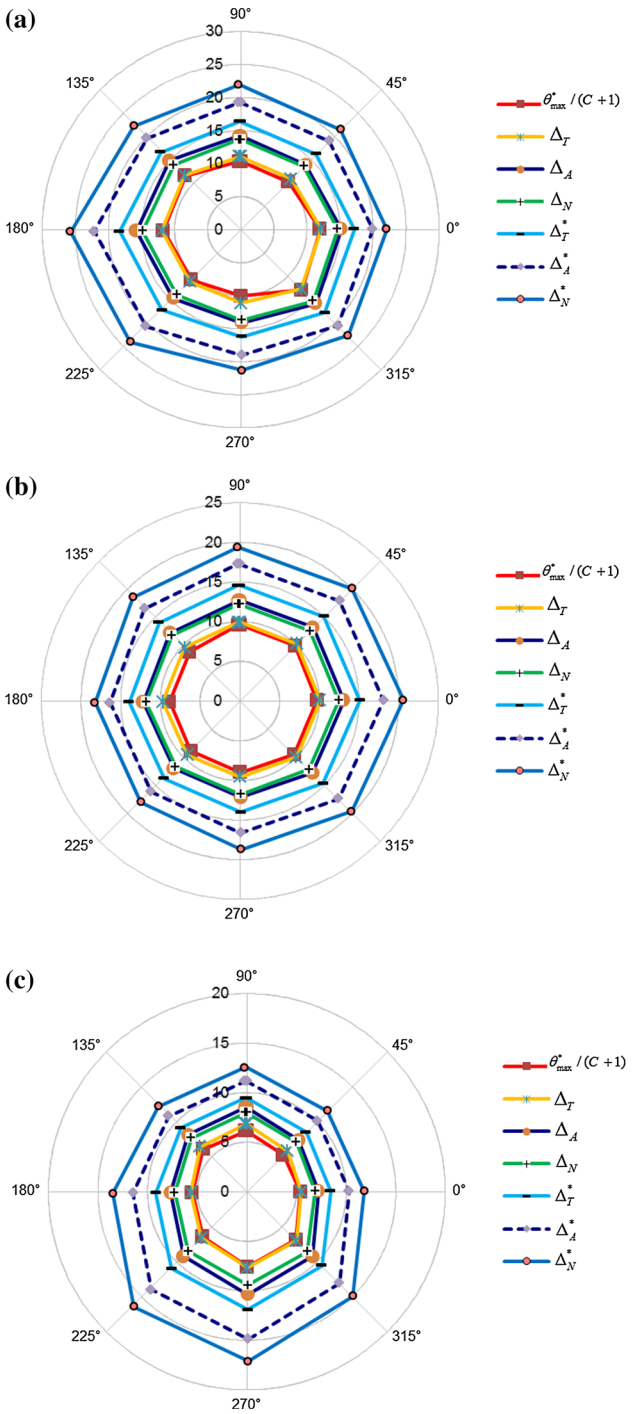

Fig. 7 Polar plots of different TIN-based roughness parameters for surfaces of S1 (**a**), S2 (**b**) and S3 (**c**)

measures for three natural rock fracture surfaces in different directions were presented.

References

Amiri Hossaini K, Babanouri N, Karimi Nasab S (2014) The influence of asperity deformability on the mechanical behavior of rock joints. Int J Rock Mech Min Sci 70:154–161. doi:10.1016/j.ijrmms.2014.04.009

Babanouri N, Karimi Nasab S, Baghbanan A, Mohamadi HR (2011) Over-consolidation effect on shear behavior of rock joints. Int J Rock Mech Min Sci 48:1283–1291. doi:10.1016/j.ijrmms.2011.09.010

Babanouri N, Karimi Nasab S, Sarafrazi S (2013) A hybrid particle swarm optimization and multi-layer perceptron algorithm for bivariate fractal analysis of rock fractures roughness. Int J Rock Mech Min Sci 60:66–74. doi:10.1016/j.ijrmms.2012.12.028

Babanouri N, Karimi Nasab S (2015) Modeling spatial structure of rock fracture surfaces before and after shear test: a method for estimating morphology of damaged zones. Rock Mech Rock Eng 48:1051–1065. doi:10.1007/s00603-014-0622-9

Barton N, Choubey V (1977) The shear strength of rock joints in theory and practice. Rock Mech 10:1–54. doi:10.1007/BF01261801

Beer AJ, Stead D, Coggan JS (2002) Estimation of the joint roughness coefficient (JRC) by visual comparison. Rock Mech Rock Eng 35:65–74. doi:10.1007/s006030200009

Bergmann D, Galanulis K, Winter D (1997) Advanced 3d fringe projection system. GOM mbH, Braunschweig

De Berg M, Van Kreveld M, Overmars M, Schwarzkopf OC (2000) Computational geometry: algorithms and applications. Springer

Grasselli G (2001) Shear strength of rock joints based on quantified surface description. Dissertation, Swiss Institute of Technology (EPFL)

Grasselli G (2006) Manuel Rocha medal recipient shear strength of rock joints based on quantified surface description. Rock Mech Rock Eng 39:295–314. doi:10.1007/s00603-006-0100-0

Grasselli G, Wirth J, Egger P (2002) Quantitative three-dimensional description of a rough surface and parameter evolution with shearing. Int J Rock Mech Min Sci 39:789–800. doi:10.1016/S1365-1609(02)00070-9

Kulatilake PHSW, Um J, Pan G (1997) Requirements for accurate estimation of fractal parameters for self-affine roughness profiles using the line scaling method. Rock Mech Rock Eng 30:181–206. doi:10.1007/BF01045716

Marache A, Riss J, Gentier S, Chiles J-P (2002) Characterization and reconstruction of a rock fracture surface by geostatistics. Int J Numer Anal Methods Geomech 26:873–896. doi:10.1002/nag.228

Odling NE (1994) Natural fracture profiles, fractal dimension and joint roughness coefficients. Rock Mech Rock Eng 27:135–153. doi:10.1007/BF01020307

Saito H, Grasselli G (2010) Geostatistical downscaling of fracture surface topography accounting for local roughness. Acta Geotech 5:127–138. doi:10.1007/s11440-010-0114-3

Tatone BSA, Grasselli G (2009) A method to evaluate the three-dimensional roughness of fracture surfaces in brittle geomaterials. Rev Sci Instrum 80:125110. doi:10.1063/1.3266964

Tse R, Cruden DM (1979) Estimating joint roughness coefficients. Int J Rock Mech Min Sci Geomech Abstr 16:303–307. doi:10.1016/0148-9062(79)90241-9

Yang ZY, Chiang DY (2000) An experimental study on the progressive shear behavior of rock joints with tooth-shaped asperities. Int J Rock Mech Min Sci 37:1247–1259. doi:10.1016/S1365-1609(00)00055-1

Yang ZY, Lo SC, Di CC (2001) Reassessing the joint roughness coefficient (JRC) estimation using Z2. Rock Mech Rock Eng 34:243–251. doi:10.1007/s006030170012